J Nanopart Res (2011) 13:7029–7039
DOI 10.1007/s11051-011-0616-4

RESEARCH PAPER

Measuring surface area of airborne titanium dioxide powder agglomerates: relationships between gas adsorption, diffusion and mobility-based methods

Ryan F. LeBouf · Bon Ki Ku · Bean T. Chen · David G. Frazer · Jared L. Cumpston · Aleksandr B. Stefaniak

Received: 1 April 2011 / Accepted: 20 October 2011 / Published online: 5 November 2011

Abstract Inhalation toxicology studies generally use the Brunauer, Emmett, and Teller (BET) gas adsorption method to measure total surface area of particles whereas occupational exposures are more readily measured by real-time mobility-based surface areas or active surface area measured with diffusion charger-based instruments. Three surface area measurement methods were studied: filter-based inert gas adsorption (BET method), diffusion charging, and mobility-based methods. The goal of the project was to investigate and develop a correlation between the measurement methods. The experimental design consisted of measuring surface area in a series of five trials for each of two powder types, fine and ultrafine titanium dioxide with primary particle sizes of 440 and 20 nm, respectively, and two aerosol concentrations. Diffusion charger instruments tended to underestimate the total particle surface area measured by the BET, but were well correlated with mobility-based surface areas obtained from a scanning mobility particle sizer. Filter-based gas adsorption methods and diffusion charging methods provide different but valuable information on total and active surface areas of particles, respectively. Results indicate they should not be used as predictors of one another.

Keywords Ultrafine titanium dioxide · Surface area · BET · Diffusion charger · Occupational health effects · EHS

R. F. LeBouf · B. T. Chen · D. G. Frazer · J. L. Cumpston · A. B. Stefaniak (✉)
National Institute for Occupational Safety and Health, Centers for Disease Control and Prevention, Morgantown, WV 26505, USA
e-mail: astefaniak@cdc.gov

B. K. Ku
National Institute for Occupational Safety and Health, Centers for Disease Control and Prevention, Cincinnati, OH 45213, USA

Introduction

Production and use of engineered nanomaterials continues to rise each year. Titanium dioxide powder (TiO_2) is among the most highly produced materials and is used in a wide variety of applications such as cosmetics, paints, and energy storage/production. Current estimates of US ultrafine TiO_2 ($uTiO_2$) powder production are ~44,000 MT/year and could reach ~260,000 MT/year by 2015 (Robichaud et al. 2009). Associated with the increased use of new technologies and science applications for $uTiO_2$ are potential risks of occupational exposure. Current mass-based occupational exposure limits for TiO_2 (total dust) range from 10 (ACGIH 2009) to 15 mg/m^3 (OSHA 2010); however, these limits may not adequately protect workers from adverse health effects associated with exposures to $uTiO_2$ (NIOSH 2011). In response to this shortcoming, the National Institute for Occupational Safety and Health (NIOSH) recently recommended two mass-based occupational exposure limits for TiO_2: 2.4 mg/m^3 for fine and 0.3 mg/m^3 for ultrafine (NIOSH 2011).

For many ultrafine and nanoscale particles, surface area is an important exposure metric as evidence exists for its relationship with deleterious health effects (Bello et al. 2009; Donaldson et al. 2000; Duffin et al. 2002; Hussain et al. 2009; Monteiller et al. 2007; Seaton et al. 2009; Stoeger et al. 2006). Surface area of ultrafine and nanoscale particles measured by gas adsorption using the Brunauer, Emmett, and Teller (BET) method, is well correlated with decreased pulmonary function in vivo and increased oxidative stress and production of reactive oxygen species in vitro (LeBlanc et al. 2010; Nurkiewicz et al. 2009; Singh et al. 2007). Ultrafine TiO_2 can trigger a pro-inflammatory response presumably due to their large surface area (Singh et al. 2007). A number of researchers concluded that for constant doses by mass, increase in particle number or surface area, measured by gas adsorption, was very likely responsible for observed adverse effects in toxicology studies (Donaldson et al. 2000; Ferin et al. 1992; Monteiller et al. 2007). Inert gas adsorption is therefore currently considered the gold standard for particle surface area measurement in conjunction with health effects studies.

Particle surface area can be measured by a variety of methods including diffusion chargers (DCs), mobility-based surface areas from measures of particle dimensions by scanning mobility particle sizers (SMPS), geometric relations using electron microscopy, and gas adsorption. Depending upon the underlying measurement principle, measured values of surface area will differ. DCs measure "active surface area", which is defined as the area of the particle that interacts with the surrounding gas or ions and is accessible only from the outside (Keller et al. 2001). SMPS measures charged particles in an air stream based on their electrical mobility diameter. Assumptions governing SMPS measurements are for individual spherical particles with unit positive charge from a bipolar equilibrium charging mechanism. SMPS number concentrations can be converted to mobility-based surface area concentrations using an internal algorithm that is based on the aforementioned assumptions. Calculations of "geometric surface area" from geometric relationships using measured particle dimensions from microscopy may be inaccurate (Weibel et al. 2005) and are less preferred than direct measurements. Gas adsorption, a direct measurement technique, relies on exposing a sample to inert gas under varying conditions of pressure to develop monolayer gas coverage. The amount of gas molecules needed to form the monolayer gas coverage and the cross-sectional area of the adsorbate gas molecule are related to the "total surface area" of the particle including pores and crevices, the latter being what differentiates it from the active surface area.

Contemporary health-based exposure assessment for nanomaterials research is focused on particle characteristics other than mass (e.g. surface area, surface chemistry, morphology) in order to identify risk factors for adverse health outcomes in exposed populations (Maynard and Aitken 2007; Maynard and Kuempel 2005). Inhalation toxicology studies generally use the gas adsorption method to measure surface area whereas occupational exposures are more readily measured by real-time DC. DCs have advantages of portability and real-time capability and are reasonably successful for nanoparticles smaller than 100 nm in recent studies (Evans et al. 2010; Heitbrink et al. 2009). A limitation of DC is that they measure only outer active surface area of particles, whereas the gas adsorption method provides a measure of total surface area of particles including pores, which has been historically used for toxicology studies. As such, development of an understanding of the relationship between these two techniques is paramount to fully understand and apply the toxicological health data to real-world occupational exposure assessments. The goal of the current project was to compare a filter-based gas adsorption (BET) method for measuring total surface area, real-time diffusion charging-based measurements of active surface area, and mobility-based surface area measurements from an SMPS. The specific aims of the project were to (1) challenge the instruments with a fine and ultrafine powder of TiO_2 at varying aerosol concentrations and (2) develop a correlation between measurements of total, active, and mobility-based surface area.

Methods

Experimental design

The experimental design consisted of collecting side-by-side measurements of the particle surface area of TiO_2 challenge aerosols using two types of diffusion chargers (DC and NSAM), a filter-based collection/gas adsorption analysis technique (BET), and an SMPS.

For the BET method, particulate was collected on Nucleopore® track-etched polycarbonate (TEPC) filters with 0.4 μm pore size (Sterlitech Corporation, Kent, WA) using 37-mm closed-face cassette samplers attached to GilAir-5 air sampling pumps (Sensidyne, Clearwater, FL) operated at 3 LPM. These filters were chosen due to their low background weight, highly reproducible background surface area, and high collection efficiency of nanoscale particles (LeBouf et al. 2011). Blank and particle-laden filter samples were degassed under light vacuum (1.9 Pa; Flovac® Degasser, Product No. 05076, Quantachrome Instruments, Boynton Beach, FL) at 120 °C for 24 h prior to analysis. Blank and particle-laden filter surface area was measured with a Quadrasorb-SI (Quantachrome Instruments) surface area analyzer and estimated from seven adsorption points collected at relative pressures in the range $p/p_0 = 0.05$–0.35; a value of 20.5 $\mathring{A}^2$ was assumed for the cross-sectional area of a krypton molecule. Each sample was measured twice for quality control. Instrument settings were: 1 min equilibration time and 0.05 torr pressure tolerance. The TiO_2 total surface area was calculated by subtracting the blank filter surface area from the TiO_2-laden filter surface area. This filter-based collection and analysis method will hereafter be referred to as BET and is a measure of the total surface area. TiO_2 powder (SRM 2001, Quantachrome Instruments) with assigned specific surface area (SSA) of 8.46 ± 0.9 m^2/g was used as a reference standard and analyzed in parallel with filter samples periodically throughout the study; the average measured SSA for this control sample was 8.16 ± 0.46 m^2/g.

The DC were a commercially available DC2000CE (DC) (Ecochem, Murrieta, CA) and a nanoparticle surface area monitor (NSAM) (Model 3550, TSI Inc., Shoreview, MN); the two instruments were operated at inlet flow rates of 1.42 and 2.5 LPM, respectively. In the DC, the sampled airborne particles are exposed to a positive ion cloud before being collected onto a filter and measuring the total charge, which is related to active surface area; this instrument gives reliable measures for particles smaller than 100 nm (Ku and Maynard 2005). The NSAM combines measurement of surface area by diffusion charging with calculations via an internationally-accepted particle lung deposition model to yield 'lung-deposited' active surface area (Fissan et al. 2007); this instrument gives reliable measures for particles smaller than 400 nm (Asbach et al. 2009). The SMPS (Model 3936, TSI, Inc.) measures mobility-derived particle size (up to 1,000 nm depending on operating conditions) and number concentration from which mobility-based surface area is calculated based on the assumption of spherical particles. It should be noted that the BET, DC and NSAM, and SMPS techniques determine surface area based on different operating principles.

Commercially available $uTiO_2$ powder (Product Type P25, Degussa AG, Hanau, Germany) was chosen for use as a model challenge material because it (1) represents a widely studied powder often used in toxicological investigations (Maier et al. 2006) and (2) this powder type is being qualified by the US National Institute of Standards and Technology as a certified reference material. An additional study material, fine titanium (IV) oxide powder, <5 μm, 99.9% + (Sigma–Aldrich, St. Louis, MO), was included in the study design to investigate the role of particle size on instrument responses. Both powders are aggregates of primary particles; the sizes of primary particles were 20 and 440 nm for the $uTiO_2$ and fine TiO_2, respectively. The volume and size distribution of mesopores (2–50 nm) in the materials was determined using gas adsorption and the Barrett-Joyner-Halenda (BJH) method. During the chamber tests, particle size distributions were monitored with a SMPS operated under the following conditions: sheath air flow rate of 3 LPM and aerosol flow rate of 0.3 LPM for $uTiO_2$ particles, and a lower sheath air flow rate of 1.7 LPM for fine TiO_2 particles was used to extend the measurable particle size range up to 1,000 nm. Mobility-based surface area values from the SMPS were compared against the diffusion charging-based and BET measures.

To simulate an animal inhalation experiment, each TiO_2 powder was aerosolized in a well-characterized laboratory system (Chen et al. 2006). The system was comprised of a fluidized-bed powder generator, cyclone, exposure cage, static discharge device and several aerosol monitoring devices (Fig. 1). A 19-liter metabolism plenum was modified for use as the exposure cage. To reduce the potential formation of agglomerates due to Van der Waals force, the $uTiO_2$ powder was carefully prepared for generation by passing through two sieves, 425 and 150 μm mesh size (to remove large agglomerates), drying (to minimize agglomerate formation due to high humidity), and storage in a sealed glass jar (to minimize agglomerate attraction through contact charges). The fine TiO_2 went through a similar process except only the 425 µm mesh size sieve was used. The fluidized-bed aerosol generator with a cyclone to remove large particles was operated at a flow rate of 10–12 LPM to disperse $uTiO_2$ powder effectively. Under these conditions, 50% aerodynamic particle size cutoff of the cyclone was approximately 3.0–3.5 µm. The cyclone was removed from the setup for dispersion of the fine TiO_2 powder. During sampling, mass concentrations were continuously monitored with a Data RAM (DR-4000 Thermo Electron Co., Franklin, MA). Four aerosol concentrations between 3 and 10 mg/m^3 were achieved by adjusting the powder feed rate in the generator. A similar mass loading between the low and high aerosol concentrations for a given powder type was obtained by adjusting the sample time. Five replicate experiments were performed at each concentration and for each powder for a total of 20 trials. Temperature, relative humidity, and pressure in the chamber were monitored throughout the sampling.

Data analyses

As noted above, the surface area measurement technique sampled at different flow rates depending upon instrument design. As such, a challenge for instrument comparison was to identify a standardized metric for comparison such as cumulative mass or sample volume. Because the concentration in the chamber was constant for a given experiment and the sample times were the same, cumulative mass collected differed among techniques. Hence, cumulative surface area was calculated using the flow rate of the instrument to make instrument values comparable. All statistical analyses were performed at $\alpha = 0.05$. A one-way ANOVA for comparison of particle modal diameter between experimental conditions was performed using Sigmaplot 9.0 (Systat Software, Inc., Chicago, IL). PROC ANOVA with Tukey's test in SAS 9.2 (SAS Institute, Cary, NC) was used to examine the statistical differences among cumulative surface area measurements. Box plots and orthogonal regressions were prepared in JMP 8.0 (SAS Institute), which is a graphic-user-interface based statistical package. Orthogonal regressions with equal variance were used to develop correlations among instruments since error components in both instrument measures (i.e. errors in both X and Y variables in the regression) are considered.

Results

Temperature and humidity for all trials were (mean ± SD): 19.5 ± 0.2 °C and 47.9 ± 0.4% RH. Average number size distributions for fine TiO_2 and $uTiO_2$ may be seen in Fig. 2a, b, respectively. The count median diameters (CMDs) obtained from the

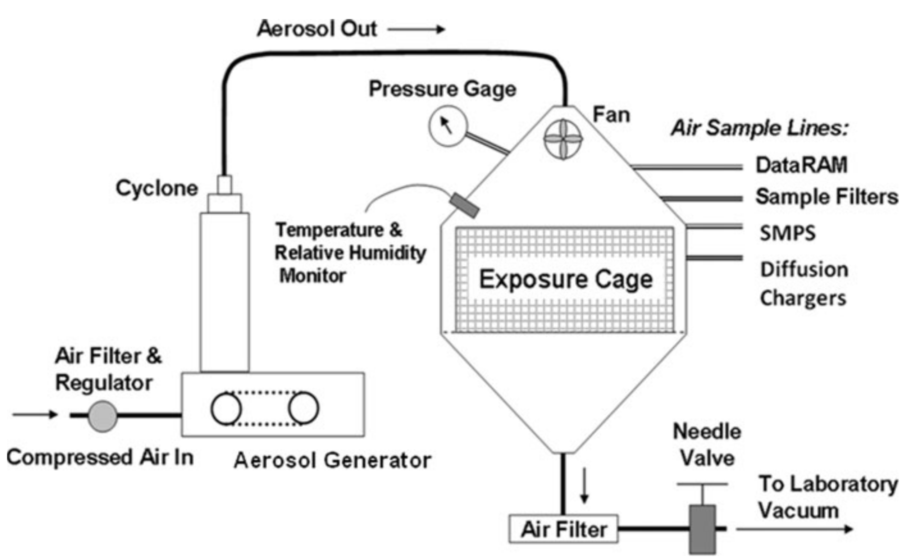

Fig. 1 Aerosol generation system schematic. Flow rates are as follows: system flow 10–12 LPM, sample filters 3 LPM, SMPS 0.3 LPM, DC 1.42 LPM, and NSAM 2.5 LPM

SMPS for $uTiO_2$ at 2.8 and 10.1 mg/m^3 were 176 (range:158–211 nm) and 205 (range:184–222 nm), respectively. The CMDs for fine TiO_2 at 3.8 and 5.0 mg/m^3 were 204 (range:106–316 nm) and 200 (range:154–264 nm), respectively. For fine TiO_2, a bimodal distribution was observed (Fig. 2a) for a number of the trials, which caused some of the modal diameter readings to be lower than expected.

Increasing the aerosol concentration did not statistically significantly change the CMDs for fine TiO_2 ($p = 1.00$), but a significant change was noticed for $uTiO_2$ ($p < 0.001$) assumedly due to agglomeration of the more numerous particles in the $uTiO_2$ aerosol. As expected the particle size distribution of $uTiO_2$ and fine TiO_2 were different based on the CMDs ($p < 0.001$). Comparing the number weighted size distribution for each of the four conditions indicated a shift in the modal diameter and a decrease in number concentration as aerosol concentration increased; this analysis demonstrated the effect of particle agglomeration.

A scanning electron microscope (SEM) image of fine TiO_2 and transmission electron microscope

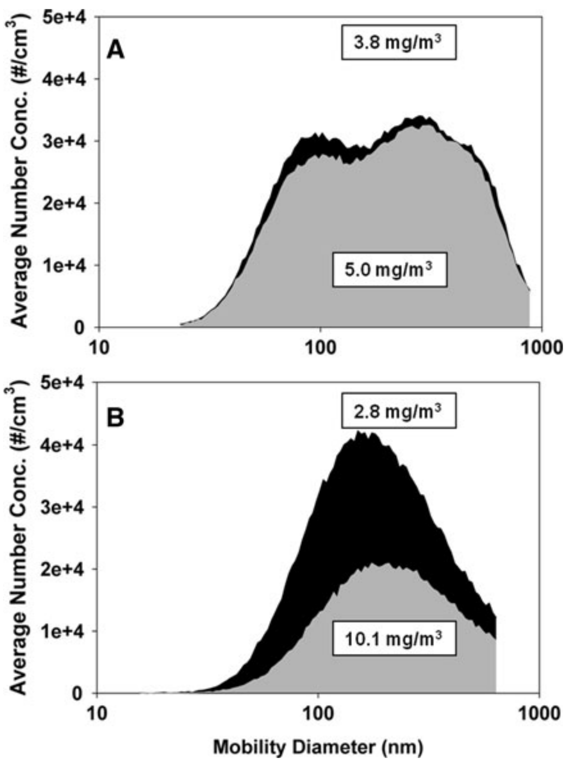

Fig. 2 Average number distribution for **a** fine TiO_2 and **b** $uTiO_2$

(TEM) image of $uTiO_2$ are displayed in Fig. 3a, b, respectively. Fine TiO_2 consisted of aggregates (fused primary particles) that were several hundred nanometers in diameter, some of which formed larger agglomerates (loosely bound by Van der Waal forces) of 1,000 nm and greater during the aerosolization process. The $uTiO_2$ was aggregates with diameters of approximately 100 nm.

The values of the coefficients of variation, which is the standard deviation divided by the mean times 100%, for measured surface area values by measurement method and aerosol condition are displayed in Table 1. Increasing aerosol concentration tended to increase variability in surface area measures except for $uTiO_2$ measured by BET. No significant differences in variability were observed among powder types for a given method.

A box plot comparison of cumulative surface area measurements for each instrument is displayed in Fig. 4a, b for fine TiO_2 and $uTiO_2$, respectively. Cumulative surface area was the sum of all measurements for the sampling period adjusted by sampling flow rate. Normalization was necessary due to the varying flow rates from 3 LPM for BET to 0.3 LPM for SMPS. Rank ordering the surface area instruments allows the end-user to easily recognize the potential relationship between various instruments. For fine TiO_2, the surface area rank order was NSAM > DC $\approx$ SMPS > BET for 3.8 mg/m^3 concentration and NSAM > DC $\approx$ SMPS $\geq$ BET for 5.0 mg/m^3 concentration. For $uTiO_2$, the rank order of measured surface area values was BET $\approx$ DC > NSAM $\approx$ SMPS for 2.8 mg/m^3 concentration and BET > DC $\approx$ NSAM $\approx$ SMPS for 10.1 mg/m^3 concentration. For the most part, lower aerosol concentrations displayed higher cumulative surface area due to higher sample volumes since sample time, and thus sample volume, was adjusted between aerosol concentrations to obtain similar mass loadings.

Instrument comparisons indicated by shared lowercase letters were based on a one-way ANOVA ($p < 0.001$). Instruments with the same lowercase letter designate no statistical difference. In the bottom of Fig. 4a, for example, the comparison of instruments measuring fine TiO_2 at a concentration of 5.0 mg/m^3 illustrated that DC and SMPS (sharing letter "c") as well as BET and DC (sharing letter "b") had no statistical difference. NSAM and SMPS, NSAM and BET, and NSAM and DC as well as BET and SMPS

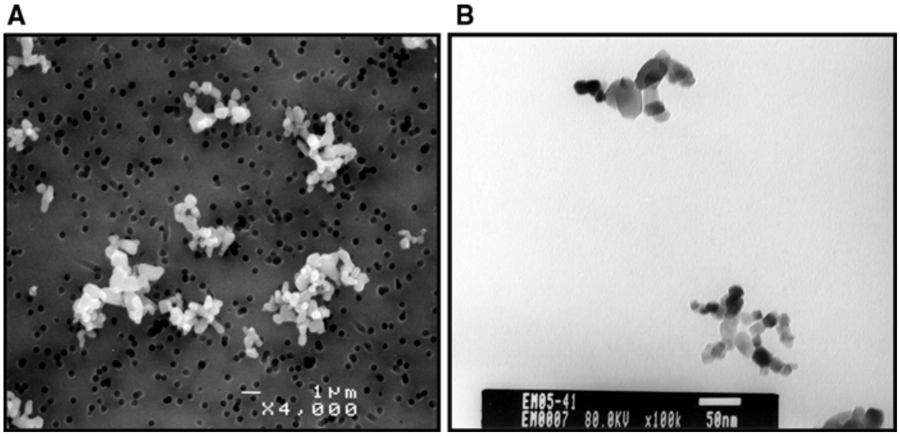

Fig. 3 **a** SEM image of fine TiO_2 and **b** TEM image of $uTiO_2$. Note: *scale bars* are different between images

Table 1 Coefficients of variation (%) for measured TiO_2 surface area values by method and aerosol condition

Method	Fine		Ultrafine	
	3.8 (mg/m^3)	5.0 (mg/m^3)	2.8 (mg/m^3)	10.1 (mg/m^3)
DC	8.9	15.7	7.5	15.2
NSAM	11.0	11.7	5.4	18.6
SMPS	10.0	12.8	10.0	12.8
BET	11.1	19.4	22.7	8.7

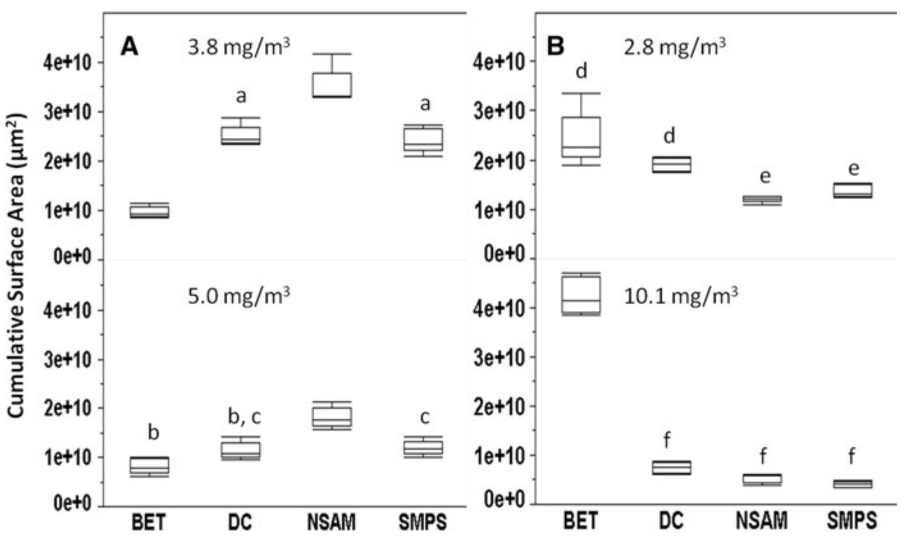

Fig. 4 Stacked box plots of **a** fine TiO_2 and **b** $uTiO_2$ cumulative surface area values from filter-based gas adsorption (BET), diffusion charger (DC), nanoparticle surface area monitor (NSAM) and scanning mobility particle sizer (SMPS). The *line* within a box is the median; the *top* and *bottom* of a box are the 75 and 25th quantiles, respectively; and the *ends* of the whiskers are maximum and minimum values that fall within the interquartile range. *Pairs of lowercase letters* indicate no statistical difference between surface area measurements based on a one-way ANOVA ($p < 0.001$). The *absence of paired lowercase letters* indicates a statistical difference for instrument types at a given powder type and concentration

were statistically different since they did not share a letter. These comparisons were made to establish whether or not there was a statistically significant difference in surface area measured by the various instruments. In the instance of statistical difference between a given set of instruments, direct comparisons between research studies or workplace exposure assessments should not be made or they should be made with an understanding of this observed difference in surface area measures. Also, it is important to remember that these techniques measure surface area based on different principles (BET-total surface area including pores, DC-total active surface area, NSAM-lung deposited surface area, and SMPS-mobility based surface area). Since the NSAM is a lung-deposited active surface area, it may be compared to the SMPS surface area when corrected for lung-deposition in the alveolar region. This analysis was performed (data not shown) and the mean surface area from the NSAM was compared to the mean SMPS-lung-deposited surface area (NSAM/SMPS-lung-deposited *100% for a given trial). For $uTiO_2$ at 2.8 and 10.1 mg/m^3, the ratio was 64.7 ± 4.2 (mean ± standard deviation) and 94.8 ± 8.6%, respectively. For fine TiO_2 at 3.8 and 5.0 mg/m^3, the ratio was 94.0 ± 4.9 and 97.4 ± 2.3%, respectively.

Figure 5 is a representative comparison of real-time surface area concentration measurements for fine TiO_2 and $uTiO_2$. Since the instruments have different measurement periods, data from the DC and NSAM (acquired every 10 s) were averaged over a 3-minute period to be comparable to the SMPS. For fine TiO_2 at 5.0 mg/m^3, the rank order for surface area concentration measurements was NSAM $>$ DC $\approx$ SMPS. The rank order for surface area concentration measurements for $uTiO_2$ at 10.1 mg/m^3 was DC $>$ NSAM $>$ SMPS. A similar trend was observed for the lower aerosol concentrations (data not shown). The rank orders for fine TiO_2 are in agreement with the box plots in Fig. 3. This was not necessarily the case for $uTiO_2$. While visually they appeared to be different, statistically there was no difference in surface area measurements between these three instruments (see Fig. 3, bottom-right panel). Active surface areas were generally higher than or equivalent to mobility-based surface areas derived from SMPS.

Table 2 summarizes orthogonal regression values for the measurement methods and powder types. The DC, NSAM and SMPS methods were well correlated as would be expected since they operate under the principle of ion attachment. DC versus SMPS for $uTiO_2$ and fine TiO_2 were the only slopes that approached unity meaning they are very good predictors of each other. An effect of powder type was evident in DC versus NSAM and NSAM versus SMPS as indicated by the changes in slope and Y-intercept values between $uTiO_2$ and fine TiO_2. The DC versus SMPS regression model did not show this effect of powder type. The regression models for BET versus all other methods demonstrate a lack of correlation. For BET method, effect of powder type was evident from the positive correlations for fine TiO_2, but negative correlations for $uTiO_2$. Increasing aerosol concentration also appeared to play a role in increasing correlations (data not shown). For $uTiO_2$, DC overestimated NSAM values by a factor of 1.72, which is intuitive since the NSAM is a lung-deposited active surface area while the DC is not. Note that these

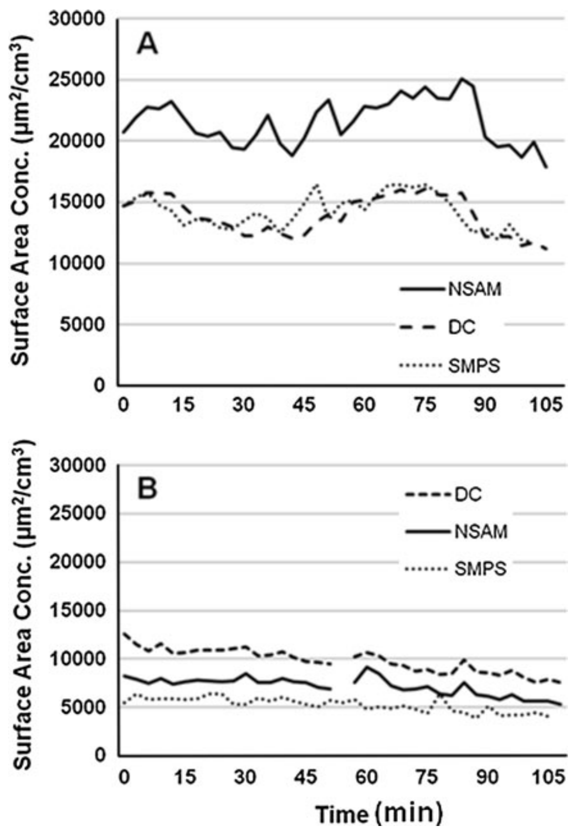

Fig. 5 Real-time surface area measurements of **a** fine TiO_2 at 5.0 mg/m^3 and **b** $uTiO_2$ at 10.1 mg/m^3 for diffusion charger (DC), nanoparticle surface area monitor (NSAM), and scanning mobility particle sizer (SMPS)

Table 2 Orthogonal regression values for instrument comparisons

Comparison	Powder	Slope	Y-intercept	Correlation[a]
DC vs. NSAM	Fine	0.792	−2.85E + 09	0.992
	Ultrafine	1.72	−1.74E + 09	0.984
	Both	0.564	5.78E + 09	0.811
DC vs. SMPS	Fine	1.11	−1.82E + 09	0.985
	Ultrafine	0.929	−3.47E + 09	0.946
	Both	1.10	−4.18E + 09	0.902
NSAM vs. SMPS	Fine	1.40	1.26E + 09	0.985
	Ultrafine	0.530	−8.43E + 08	0.950
	Both	2.58	−2.90E + 09	0.540
BET vs. DC	Fine	0.077	7.56E + 09	0.366
	Ultrafine	−1.82	5.74E + 10	−0.858
	Both	−3.14	7.05E + 10	−0.543
BET vs. NSAM	Fine	0.062	7.32E + 09	0.377
	Ultrafine	−3.17	6.09E + 10	−0.887
	Both	−1.35	4.50E + 10	−0.770
BET vs. SMPS	Fine	0.083	7.45E + 09	0.357
	Ultrafine	−1.66	6.32E + 10	−0.883
	Both	−6.17	1.32E + 11	−0.294

[a] Correlation is the Pearson product-moment correlation coefficient

regressions should only be used for a rudimentary understanding of instrument response to varying aerosol conditions and not as a means of predicting one variable from another since they are based on only two nominal aerosol concentrations and two powder types.

Table 3 summarizes the method comparisons by ratios of cumulative surface area by powder type and aerosol concentration. DC versus NSAM, for example, is the cumulative surface area measured by the DC divided by that measured by the NSAM. These ion-attachment methods displayed very consistent ratios that appeared to be affected by powder type but not by aerosol concentration. DC versus NSAM ratios changed from 0.7 to 1.6 when changing from fine TiO_2 to $uTiO_2$. DC versus SMPS ratios exhibited a small change from 1.04 to 0.95 with an increase in the aerosol concentration. BET ratios with all other instruments were affected by powder type and aerosol concentration. The ratios for BET versus all other instruments for $uTiO_2$ at 10.1 mg/m^3 displayed the most dramatic differences (5.77–10.5) indicating an underestimation of surface area measures by diffusion chargers (DC and NSAM) and mobility-based surface area (SMPS) compared to the BET method.

Discussion

The trend of lower surface area for higher concentrations of $uTiO_2$, illustrated in Fig. 3b, is less pronounced for the alternative measurement techniques compared to BET. Because BET uses inert gas adsorption to measure the total surface area, the values are higher than the active surface area measured by DC and NSAM or the mobility-based surface area derived from SMPS. This may be influenced by the measurement range of the instruments (e.g. SMPS only measured particles smaller than 1,000 nm). The mean lung-deposited mobility-based surface area calculated from the SMPS was roughly equivalent to the mean NSAM surface area in three out of four conditions. For uTiO2 at 2.8 mg/m^3, the NSAM was roughly 64% of the SMPS-lung-deposited surface area which may be due to particle morphology and size affecting the determination of electrical mobility diameter by the SMPS (i.e. incorrectly classified size of aggregate particles). Also, the assumption of spherical particles made by the SMPS for calculating surface area may cause an over prediction of surface area of aggregates (Lall and Friedlander 2006; Lall et al. 2006). The reason that the DC-measured surface

Table 3 Average method ratios (±two standard deviations) of cumulative surface area by TiO_2 powder type and aerosol concentration

Method ratio	Fine		Ultrafine	
	3.8 (mg/m^3)	5.0 (mg/m^3)	2.8 (mg/m^3)	10.1 (mg/m^3)
DC vs. NSAM	0.72 ± 0.02	0.63 ± 0.05	1.58 ± 0.12	1.41 ± 0.11
DC vs. SMPS	1.04 ± 0.07	0.95 ± 0.06	1.40 ± 0.06	1.82 ± 0.05
NSAM vs. SMPS	1.45 ± 0.10	1.52 ± 0.03	0.89 ± 0.06	1.30 ± 0.12
BET vs. DC	0.39 ± 0.07	0.75 ± 0.21	1.27 ± 0.28	5.77 ± 0.58
BET vs. NSAM	0.28 ± 0.05	0.46 ± 0.10	2.03 ± 0.58	8.16 ± 1.27
BET vs. SMPS	0.41 ± 0.09	0.70 ± 0.16	1.8 ± 0.49	10.52 ± 0.93

area is lower than BET surface area may be due to several factors including particle size and porosity. The actual median diameter of the $uTiO_2$ is larger than 100 nm although the primary particle size is 20 nm and the agglomerates have relatively compact structure. Recent studies showed that the DC can give particle surface area comparable to its geometric surface area as measured by TEM for silver nanoparticles smaller than 100 nm, but in the size range over 100 nm, it underestimates the geometric surface area (Ku and Maynard 2005). The DC-based surface area deviates significantly from the geometric surface area as the particle size increases up to 900 nm for spherical particles (Ku 2009, 2010). The diffusion charging mechanism depends on a number of parameters such as particle structure, ion concentrations, and ion properties. If particle pore size is much smaller than the mean free path of ions ($\sim$15 nm in 10% humid air (Pui 1976), the chance of ions to get access to the pore may be less than that for pores larger than the mean free path because ions could hit other particle surface before they enter the pore. The volume and size distribution of pores in the $uTiO_2$ material, determined from the desorption branch of isotherms using the BJH method, were 0.113 cm^3/g and 3.2 nm, respectively. Hence, charging mechanism explains a portion of the difference between DC- and BET-measured surface areas.

The variability of fine TiO_2 measurements among instruments may be due to the following factors: BET surface area measures were low since particle loading corresponded to surface area measures around the LOD of 0.02 m^2; and NSAM overestimated surface area of fine TiO_2 compared to the other surface area measures presumably due to the deviation of required response function from instrument response function for particles with diameters >400 nm (Asbach et al. 2009). NSAM has been shown to give reliable measures of active surface area for particles with diameters <400 nm (Asbach et al. 2009). DC active surface area values are comparable to surface area values derived from number distributions using SMPS, illustrated in Table 2. Since surface area values from SMPS and NSAM surface area values are dependent on calibration using individual (or singlet) spherical or agglomerate particles, the instrument response to irregularly shaped particles with different primary particle sizes such as TiO_2 agglomerates is unpredictable. Some researchers have attempted to provide a theoretical conversion of surface areas obtained by electrical mobility analyzers for ultrafine aggregates (Lall and Friedlander 2006) and also attempted to assess the effect of particle morphology on DC for nanoparticle agglomerates (Shin et al. 2010). Ku and Kulkarni (2010, 2011) investigated the effect of particle structure on surface area measurement from the DC and SMPS for agglomerates in the sub micrometer size range. They showed that the SMPS-estimated surface area is close to geometric surface area measured based on mass and primary particle size for open agglomerates and it becomes lower than that for compact agglomerates while the DC measurements underestimate geometric surface area for all types of agglomerates. It is suspected that the DC instrument is more sensitive to particle size than particle structure based on previous studies, presumably due to the fact that ion attachment is mainly correlated with the outer surface area of the particle.

Conclusions

Based on the orthogonal correlation coefficients, DC and SMPS are good predictors of each other for both fine TiO_2 and $uTiO_2$ as are NSAM and SMPS for $uTiO_2$. BET and ion-attachment methods were affected by powder type and concentration. The BET surface area was not correlated with near real-time surface area measurements from a DC, NSAM, or SMPS (see Table 2). Hence, no concrete predictive relationship could be derived among these measures of total, active, and geometric surface area. Future research will attempt to elucidate this relationship with regard to effects of particle agglomeration, temperature and relative humidity. BET total surface area, however, was observed to overestimate active (DC and NSAM) and mobility-based (SMPS) surface areas for $uTiO_2$ (see Table 3). NSAM underestimated DC surface area for $uTiO_2$, but overestimated for fine TiO_2 (see Table 3). The absence of a meaningful relationship among measures of total surface area (BET) used in toxicological studies and active surface area (DC or NSAM) used in occupational exposure assessments remains a significant barrier to translating animal toxicology data to meaningful worker protection practices. As an example, if a worker was sampled with a DC in the field to measure active surface area exposure to nanoparticles, an underestimation of the BET total surface area measure would be observed. Since BET is currently used for toxicology studies, health-based outcomes are generated with a higher measure of surface area (i.e. BET overestimates surface area measure compared with DC) than would be seen in the field, leading to an underestimation of risk to the employee.

Currently, BET values of surface area for bulk powder ("as produced") are provided for inhalation toxicology studies, but the measured surface area may change due to aerosolization (or agglomeration due to aerosolization). The "as administered" surface area should be considered when correlating exposure with health outcomes (Oberdorster et al. 2005). For $uTiO_2$, DC-type instruments will underestimate the total surface area measured by BET, but they provide useful real-time industrial hygiene information for the evaluation and control of aerosol-producing processes. In a homogenous exposure environment, filter-based BET method may provide the best information for a time-weighted average exposure over an employee's work shift or an animal exposure study. Hence, the use of a particular surface area measuring instrument should be based on the scenario (expected particle size, morphology, concentration, etc.) and goals of the sampling.

Acknowledgments The authors would like to thank Arthur L. Miller and Ji Young Park for their thorough review of this manuscript. The findings and conclusions in this report are those of the authors and do not necessarily represent the views of the National Institute for Occupational Safety and Health.

References

ACGIH (2009) 2009 TLVs® and BEIs® based on the documentation of the threshold limit values for chemical substances and physical agents and biological exposure indices. American Conference of Governmental Industrial Hygienists, Cincinnati, OH

Asbach C, Fissan H, Stahlmecke B, Kuhlbusch TAJ, Pui DYH (2009) Conceptual limitation and extensions of lung-deposited nanoparticle surface area monitor (NSAM). J Nanopart Res 11:101–109

Bello D, Hsieh SF, Schmidt D, Rogers E (2009) Nanomaterials properties vs. biological oxidative damage: implications for toxicitiy screening and exposure assessment. Nanotoxicology 3:249–261

Chen B, Frazer D, Stone S, Schwegler-Berry D, Cumpston J, McKinney W, Lindsley W, Frazer A, Donlin M, Vandestouwe K, Castranova V (2006) Development of a small inhalation system for rodent exposure to fine and ultrafine titanium dioxide aerosols. In: Biswas P, Chen D-R, Hering S (eds) Proceedings of the Seventh International Aerosol Conference. American Association for Aerosol Research, St. Paul, pp 858–859

Donaldson K, Stone V, Gilmour PS, Brown DM, MacNee W (2000) Ultrafine particles: mechanisms of lung injury. Philos Trans 358(1775):2741–2749

Duffin R, Tran CL, Clouter A, Brown DM, MacNee W, Stone V, Donaldson K (2002) The importance of surface area and specific reactivity in the acute pulmonary inflammatory response to particles. Ann Occ Hyg 46(Suppl 1):242–245

Evans DE, Ku BK, Birch ME, Dunn KH (2010) Aerosol monitoring during carbon nanofiber production: mobile direct reading sampling. Ann Occ Hyg 54:514–531

Ferin J, Oberdorster G, Penney DP (1992) Pulmonary retention of ultrafine and fine particles in rats. Am J Respir Cell Mol Biol 6:535–542

Fissan H, Neumann S, Trampe A (2007) Rationale and principle of an instrument measuring lung deposited nanoparticle surface area. J Nanopart Res 9:53–59

Heitbrink WA, Evans DE, Ku BK, Maynard AD, Slavin T, Peters T (2009) Relationship among particle number, surface area, and respirable mass concentration in an automotive engine manufacturing. J Occ Environ Hyg 6:19–31

Hussain S, Boland S, Baeza-Squiban A, Hamel R, Thomassen LCJ, Martens JA, Billon-Galland MA, Fleury-Feith J, Moisan F, Pairon JC, Marano F (2009) Oxidative stress and proinflammatory effects of carbon black and titanium dioxide nanoparticles: role of particle surface area and internalized amount. Toxicol 260:142–149

Keller A, Fierz M, Siegmann K, Siegmann H, Filippov A (2001) Surface science with nanosized particles in a carrier gas. J Vac Sci Technol 19:1–8

Ku BK (2009) Diffusion charger based aerosol surface area monitor response to airborne spherical particles 100–800 nm in diameter. In: Abstracts of the 4th international conference on nanotechnology-occupational and environmental health. Helsinki, Finland

Ku BK (2010) Determination of the ratio of diffusion charging based surface area to geometric surface area for spherical particles in the size range of 100–900 nm. J Aerosol Sci 41:835–847

Ku BK, Kulkarni P (2010) Comparison of different approaches for measurement of surface area of nanoaerosols. The AAAR conference, Portland

Ku BK, Kulkarni P (2011) Comparison of diffusion charging and mobility based methods for measurement of aerosol surface area (Personal communication)

Ku BK, Maynard AD (2005) Comparing aerosol surface area measurement of monodisperse ultrafine silver agglomerates using mobility analysis, transmission electron microscopy and diffusion charging. J Aerosol Sci 36:1108–1124

Lall AA, Friedlander SK (2006) On-line measurement of ultrafine aggregate surface area and volume distributions by electrical mobility analysis: I. Theoretical analysis. J Aerosol Sci 37:260–271

Lall AA, Seipenbusch M et al (2006) On-line measurement of ultrafine aggregate surface area and volume distributions by electrical mobility analysis: II. Comparison of measurements and theory. J Aerosol Sci 37:272–282

LeBlanc A, Moseley A, Chen B, Frazer D, Castranova V, Nurkiewicz T (2010) Nanoparticle inhalation impairs coronary microvascular reactivity via a local reactive oxygen species-dependent mechanism. Cardiovasc Toxicol 10:27–36

LeBouf RF, Stefaniak AB, Chen BT, Frazer DG, Virji MA (2011) Measurement of airborne nanoparticle surface area by gas adsorption during inhalation toxicology experiments. Nanotoxicology. doi:10.3109/17435390.2010.546951

Maier M, Hannebauer B, Holldorff H, Albers P (2006) Does lung surfactant promote disaggregation of nanostructured titanium dioxide? J Occ Environ Med 48:1314–1320

Maynard AD, Aitken RJ (2007) Assessing exposure to airborne nanomaterials: current abilities and future requirements. Nanotoxicology 1:26–41

Maynard AD, Kuempel ED (2005) Airborne nanostructured particles and occupational health. J Nanopart Res 7:587–614

Monteiller C, Tran L, MacNee W, Faux S, Jones A, Miller B, Donaldson K (2007) The pro-inflammatory effects of low-toxicity low-solubility particles, nanoparticles and fine particles, on epithelial cells in vitro: the role of surface area. J Occ Environ Med 64:609–615

NIOSH (2011) National Institute for Occupational Safety and Health Current Intelligence Bulletin 63: Evaluation of health hazard and recommendations for occupational exposure to titanium dioxide. DHHS Publication No. 2011-160. http://www.cdc.gov/niosh/docs/2011-160/pdfs/2011-160.pdf. Accessed 30 Aug 2011

Nurkiewicz T, Porter D, Hubbs A, Stone S, Chen B, Frazer D, Boegehold M, Castranova V (2009) Pulmonary nanoparticle exposure disrupts systemic microvascular nitric oxide signaling. Toxicol Sci 110:191–203

Oberdorster G, Maynard A, Donaldson K, Castranova V, Fitzpatrick J, Ausman K, Carter J, Karn B, Kreyling W, Lai D, Olin S, Monteiro-Riviere N, Warheit D, Yang H (2005) Principles for characterizing the potential human health effects from exposure to nanomaterials: elements of a screening strategy. Part Fibre Toxicol 2:1–35

OSHA (2010) Occupational safety and health association. Permissible exposure limits. General Industry- Total Dust, CFR 1910.1000 Table Z-1

Pui D (1976) Experimental study of diffusion charging of aerosols. PhD thesis, University of Minnesota

Robichaud C, Uyar A, Darby M, Zucker L, Wiesner M (2009) Estimates of upper bounds and trends in nano-TiO2 production as a basis for exposure assessment. Environ Sci Technol 43:4227–4233

Seaton A, Tran L, Aitken R, Donaldson K (2010) Nanoparticles, human health hazard and regulation. J R Soc Interface 7(Suppl 1):S119–S129

Shin WG, Wang J, Mertler M, Sachweh B, Fissan H, Pui DYH (2010) The effect of particle morphology on unipolar diffusion charging of nanoparticle agglomerates in the transition regime. J Aerosol Sci 41:975–986

Singh S, Shi T, Duffin R, Albrecht C, van Berlo D, Hohr D, Fubini B, Martra G, Fenoglio I, Borm PJA, Schins RPF (2007) Endocytosis, oxidative stress and IL-8 expression in human lung epithelial cells upon treatment with fine and ultrafine TiO_2: role of the specific surface area and of surface methylation of the particles. Toxicol Appl Pharmacol 222:141–151

Stoeger T, Reinhard C, Takenaka S, Schroeppel A, Karg E, Ritter B, Heyder J, Schulz H (2006) Instillation of six different ultrafine carbon particles indicates a surface area threshold dose for acute lung inflammation in mice. Environ Health Perspect 114:328–333

Weibel A, Bouchet R, Knauth P (2005) The big problem of small particles: a comparison of methods for determination of particle size in nanocrystalline anatase powders. Chem Mater 17:2378–2385